J Mater Sci: Mater Electron (2016) 27:10082–10088
DOI 10.1007/s10854-016-5082-4

# Fabrication of $SiO_2/TiO_2$ double layer thin films with self-cleaning and photocatalytic properties

**Hemraj M. Yadav**[1] · **Jung-Sik Kim**[1]

Received: 25 January 2016 / Accepted: 27 May 2016 / Published online: 6 June 2016


**Abstract** Transparent antireflective $SiO_2/TiO_2$ double layer thin films were prepared using a sol–gel method and deposited on glass substrate by spin coating technique. Thin films were characterized using XRD, FE-SEM, AFM, UV–Vis spectroscopy and water contact angle measurements. XRD analysis reveals that the existence of pure anatase phase $TiO_2$ crystallites in the thin films. FE-SEM analysis confirms the homogeneous dispersion of $TiO_2$ on $SiO_2$ layer. Water contact angle on the thin films was measured by a contact angle analyzer under UV light irradiation. The photocatalytic performance of the $TiO_2$ and $SiO_2/TiO_2$ thin films was studied by the degradation of methylene blue under UV irradiation. The effect of an intermediate $SiO_2$ layer on the photocatalytic performance of $TiO_2$ thin films was examined. $SiO_2/TiO_2$ double layer thin films showed enhanced photocatalytic activity towards methylene blue dye.

## 1 Introduction

The photocatalysis technology is a promising alternative for environmental remediation because a global pollution has recognized to be a serious problem that needs to be addressed immediately [1, 2]. Titanium dioxide ($TiO_2$) is an important semiconducting material with extraordinary physical and chemical properties. $TiO_2$ is a versatile material and its photocatalytic properties have been utilized in various applications to remove contaminants from air and water and killing of harmful bacteria and cancer cells [3–6]. $TiO_2$ is widely used as pigments, sunscreen, paints, toothpaste, ointments, electrochemical electrodes, capacitors, and solar cells [7, 8]. To extend its applicability in self-cleaning surfaces, many researchers have been developing various ways to apply $TiO_2$ coating on different substrates [9].

Silica-titania ($SiO_2$–$TiO_2$) based coatings have gained extensive interest for optics application, including antireflective coatings and optical planar waveguides, due to their high, photoactivity, strong redox property, high thermal stability, high chemical durability, low thermal expansion coefficient, versatile refractive index and hydrophilicity [10, 11].

$TiO_2$ coatings have a wide range of applications in catalysis, self-cleaning, antifogging, optics, flexible displays, biomedical, energy generation, decorative and barrier coatings for pharmaceutical and food products [12, 13]. Various metals, insulators, and semiconductors are mostly used to prepare thin film coatings. Thin films prepared from semiconducting metal oxides are well transparent in a broad wavelength range and have low ($MgF_2$, $SiO_2$), moderate ($Al_2O_3$, $Ta_2O_5$) or high ($TiO_2$, $Nb_2O_5$) refraction index [12].

Anatase $TiO_2$ is more appropriate for photochemical transformation application because of its high efficiency, non-toxicity, strong oxidizing power, high photochemical stability and exhibit a photo-induced super hydrophilicity under UV light irradiation [11, 14]. This photo-induced super hydrophilicity allows removing surface adsorbed organic pollutants without any detergent [11]. The main advantage of $TiO_2$ is that the photocatalysis and hydrophilicity can occur simultaneously on the same

✉ Jung-Sik Kim
jskim@uos.ac.kr

Hemraj M. Yadav
hemrajy@gmail.com

[1] Department of Materials Science and Engineering, University of Seoul, Seoul 02504, South Korea

surface even though the mechanisms are completely different [15].

Metal oxide thin films have been extensively used as anti-reflection, protective and self-cleaning coatings depending on their particular chemical composition and micromorphology [13]. Various methods have been developed to prepare thin films such as sol–gel [16], hydrothermal [17], chemical vapor deposition [18], sputtering [19], electrodeposition [20], chemical bath deposition [21], etc. Among these techniques, the sol–gel method has many advantages of relatively simple, inexpensive, low temperature, easy to control process parameters, homogeneity and well dispersion of $TiO_2$ [22, 23].

Preparing a homogenous $SiO_2/TiO_2$ double layer is considered as a real challenge due to the cracks or delamination's on the surface or interface of the films and more hydrophilic nature of $SiO_2$ layer affects the quality of the produced films. Thus, in order to prepare homogeneous double layer thin films, removal of residual alkoxy groups is required [23]. Several methods have been used to eliminate residual alkoxy groups including, UV light illumination, plasma cleaning and thermal treatment for fabricating multilayer films [23–25]. Here an attempt was made to develop a good self-cleaning coating which also exhibits efficient photocatalytic activity.

In the present work, uniform $TiO_2$, $SiO_2$, and $SiO_2/TiO_2$ thin films were prepared by sol–gel spin coating on a glass substrate. The films were analyzed by X-ray diffraction, Field emission scanning electron microscopy (FE-SEM), atomic force microscopy (AFM) and UV–Vis spectroscopy. Photo-induced hydrophilicity of the thin films was studied by measuring the water contact angle before and after UV irradiation. The unique physiochemical properties of $TiO_2$ were used to evaluate the photocatalytic activity and super hydrophilicity of the self-cleaning thin films. The photocatalytic degradation of methylene blue dye over thin films was estimated using a UV–Vis spectrophotometer.

## 2 Experimental

### 2.1 Preparation of thin films

The $SiO_2$, $TiO_2$, $SiO_2/TiO_2$ double layer films were prepared by the sol–gel method at room temperature. Figure 1 shows the flow chart of the preparation of thin films. Prior to coating, the glass substrates were ultrasonically cleaned in acetone and ethanol, respectively. Initially, $SiO_2$ sol and $TiO_2$ sol were prepared separately. A $SiO_2$ sol was prepared by hydrolyzing tetraethyl orthosilicate (TEOS) with ethanol and deionized water in the presence of $HNO_3$ catalyst under magnetic stirring for 1 h. The molar ratio of TEOS:Ethanol:$H_2O$:$HNO_3$ was 1:13.5:11.5:0.3. A small quantity of surfactant Triton X-100 (2 wt%) was added to this mixture. Then, cleaned glass substrates were spin-coated by the $SiO_2$ precursor sol (100 μL) with the rotation speed of 2000 rpm for 20 s. Then, the coatings were dried at room temperature and then heat-treated at 400°C for 1 h, at a heating rate of 10°C/min. Then, a $TiO_2$ sol was prepared by mixing titanium tetra-isopropoxide (TTIP) with ethanol in the presence of $HNO_3$ and deionized water and the relative molar ratio of each chemical in the precursor sol was TTIP:Ethanol:$HNO_3$:$H_2O$ = 1:18.5:16:2.2. After magnetically stirring for 1 h in a glass beaker, $TiO_2$ sol (100 μL) was deposited on the glass substrates with the rotation speed of 2000 rpm for 20 s. Then, the glass substrates were heat treated at 400°C for 1 h, at a heating rate of 10°C/min.

The double layer film was performed on previously fabricated $SiO_2$ thin film by spin coating technique. The $TiO_2$ sol (100 μL) was deposited on the $SiO_2$ thin film with the rotation speed of 2000 rpm for 20 s. Finally, the double layer thin films were heat treated at 400°C for 1 h, at a heating rate of 10°C/min.

### 2.2 Characterization

X-ray diffractometer (Bruker D8 advance, Germany, CuKα (λ = 1.54056 Å) was used to investigate crystalline phase of thin films. Surface hydrophilicity of the films was performed at room temperature using a goniometer (Surface tech, GSTD, Korea) attached to a camera. Water contact angles were measured on the thin film surface by dropping water droplets (2 μL) at pH 7.0. The photo-induced hydrophilicity of the films was measured using a UV lamp (Daytime CFL 20W Blacklight, Korea). A field-emission scanning electron microscopy (FE-SEM, Hitachi Field Emission S-4300) was used to observe surface morphologies and the cross section of the thin films. The thickness of the thin films was evaluated by an FE-SEM cross section method. Surface observation of thin films was carried out by atomic force microscopy (AFM, XE-100 Park system, Korea). AFM images were analyzed using XEI program software. UV–Vis transmission spectra of the thin films were recorded on a UV–Vis spectrophotometer (S-4100 PDA Scinco, Korea).

### 2.3 Photocatalytic activity

The photocatalytic activity of the thin films was studied using degradation of MB solution under UV light irradiation. 10 mL of MB aqueous solution with the concentration of $5.34 \times 10^{-6}$ M was taken in a small beaker. The $TiO_2$ coated glass substrates (2.5 × 2.5 cm) were dipped into the MB solution horizontally. Before irradiation, the beaker was kept in the dark under magnetic stirring for 1 h to

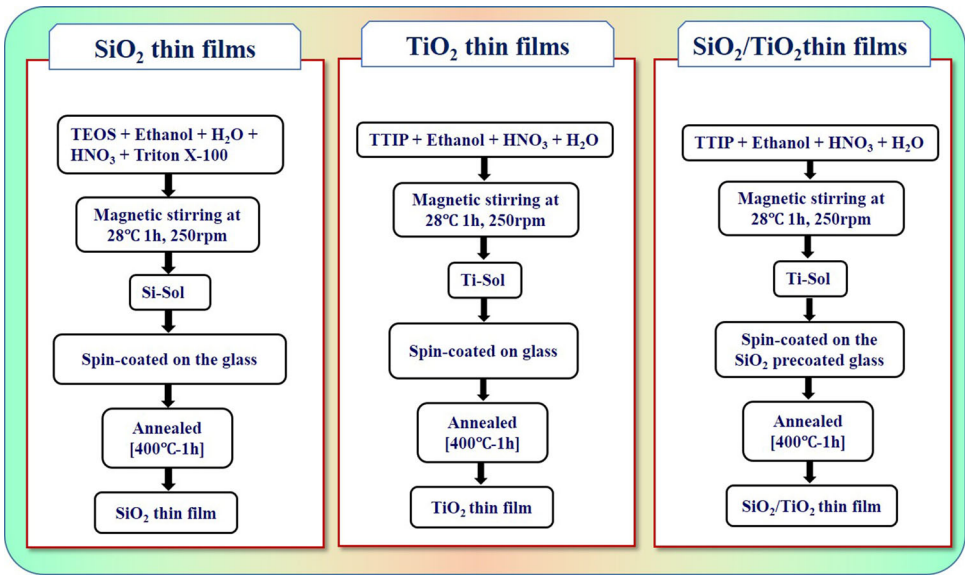


**Fig. 1** Flow chart of the preparation of $SiO_2$, $TiO_2$ and $SiO_2/TiO_2$ thin films

ensure adsorption–desorption equilibrium. Then, this beaker was irradiated by a 20 W UV lamp (Daytime CFL 20W Blacklight, Korea.). The distance from the lamp to the surface of the solution was 7 cm. The concentration of MB aqueous solution was determined every 60 min with a UV–Vis spectrophotometer.

## 3 Results and discussion

### 3.1 Structural analysis

The XRD patterns of $SiO_2$, $TiO_2$ and $SiO_2/TiO_2$ thin films deposited on a glass substrate are shown in Fig. 2. The XRD pattern of $SiO_2$ thin films (Fig. 2a) reveals that there

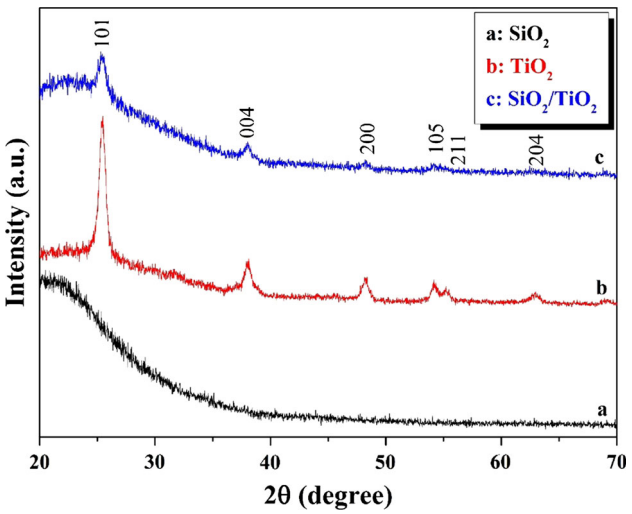


**Fig. 2** XRD patterns of $SiO_2$, $TiO_2$, and $SiO_2/TiO_2$ thin films

are no any characteristic peaks of $SiO_2$. The diffraction pattern of $SiO_2$ exhibits a broad peak in the range 2θ of 10°–40° indicates the amorphous nature of $SiO_2$ thin films. The well-defined reflection of both thin films ($TiO_2$ and $SiO_2/TiO_2$) could be indexed to anatase phase. The diffraction peaks of both thin films located at $2\theta = 25.27°$, 37.91°, 48.17°, 53.89°, 54.99° and 62.48° can be indexed to the planes 101, 004, 200, 105, 211 and 204 of anatase $TiO_2$ (JCPDS 21-1272). This indicates that $TiO_2$ is well dispersed on $SiO_2$ layer and crystallite size is appropriate for the detection by XRD. No other phases such as rutile or brookite were observed. The average crystallite size was calculated from the Scherrer's equation using the broadening of the (1 0 1) anatase reflection. The average crystallite sizes of nanoparticles for $TiO_2$ and $SiO_2/TiO_2$ thin films were about 13 and 16 nm, respectively. Thus, XRD analysis confirms the existence of anatase phase, which is considered as most suitable for the photocatalytically active phase of $TiO_2$ [14, 22, 26].

### 3.2 Morphological analysis

Figure 3a–c shows the FESEM micrographs of the $SiO_2$, $TiO_2$, and $SiO_2/TiO_2$ thin films. All films are homogeneous and without cracks over a wide area. The $SiO_2$ thin film has flat texture and consists of very fine particles. For $TiO_2$ thin film, the dispersion of $TiO_2$ grains was less tightly packed and a significant grain growth was noticed. In contrast, the $SiO_2/TiO_2$ double layer is composed of densely packed and uniform nanoscale grains (10–15 nm) of $TiO_2$ layer. From FESEM micrographs shown in Fig. 3, it can be observed that the $TiO_2$ grains were embedded on $SiO_2$ layer which forms homogenous $SiO_2/TiO_2$ double layer thin films. No

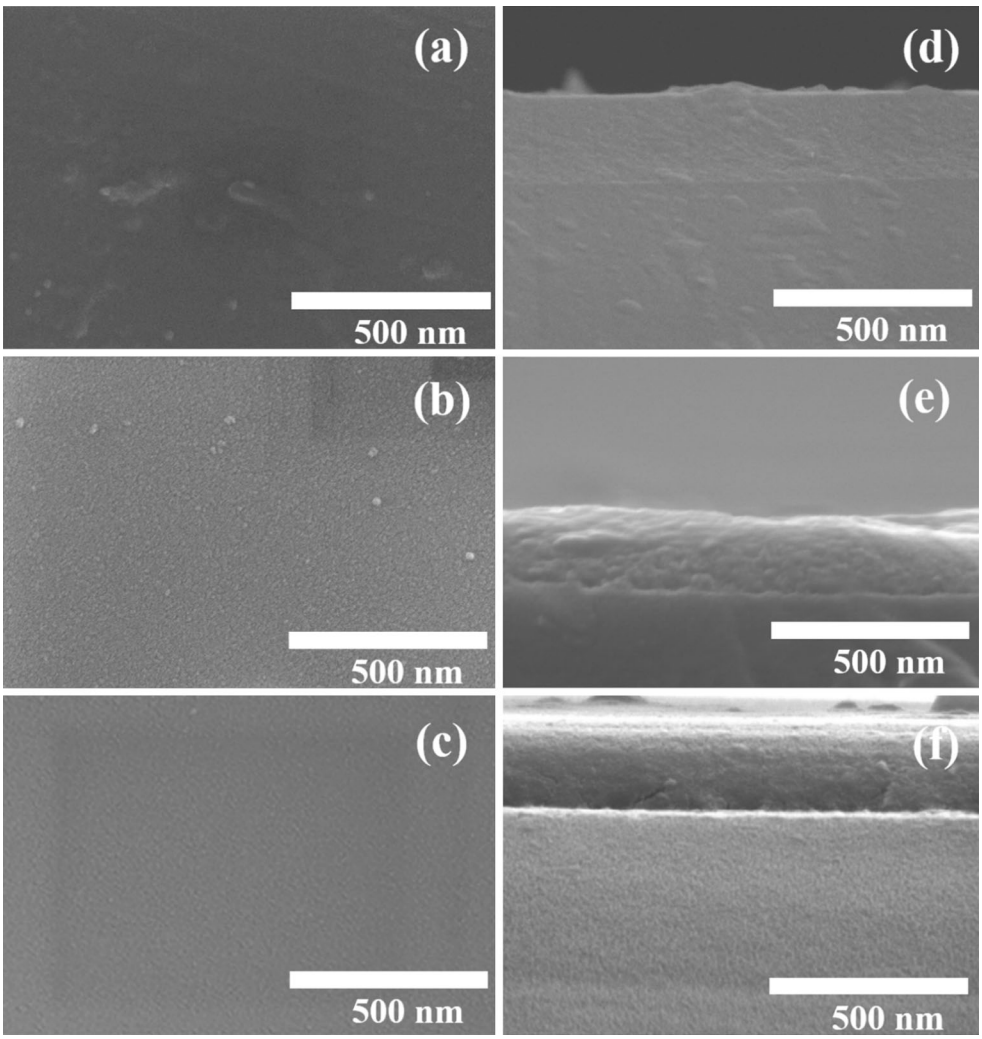


**Fig. 3** FE-SEM images of **a** $SiO_2$, **b** $TiO_2$, and **c** $SiO_2/TiO_2$ and cross-sectional view of **d** $SiO_2$, **e** $TiO_2$, and **f** $SiO_2/TiO_2$ thin films

any separate $SiO_2$ and $TiO_2$ clusters were observed in double thin films.

Figure 3d–f shows cross-sectional SEM micrographs for $SiO_2$, $TiO_2$ and $SiO_2/TiO_2$ thin films. The average thickness of the thin films was estimated according to an FE-SEM cross section. The thickness for the $SiO_2$, $TiO_2$, and $SiO_2/TiO_2$ thin films was about 260, 175 and 420 nm, respectively. The cross-sectional analysis confirms the formation of uniform structures.

Figure 4 shows the three-dimensional AFM images of $SiO_2$, $TiO_2$ and $SiO_2/TiO_2$ thin films deposited on the glass substrate. The arithmetic roughness ($R_a$) and the root-mean-square roughness ($R_{rms}$), were calculated using the topographical data and listed in Table 1. According to the AFM images, the root mean square roughness values ($R_{rms}$) of the $SiO_2$, $TiO_2$, and $SiO_2/TiO_2$ thin films are 0.1378, 0.998 and 1.219 nm, respectively. The surface skewness ($R_{sk}$) of the $TiO_2$ thin film is positive which confirms the presence of few bumps, whereas a negative value of $R_{sk}$ indicates that the surface is made up of valleys [27, 28]. The distribution of the sample height can be obtained from Kurtosis ($R_{ku}$) value [28]. The AFM analysis indicates that the $SiO_2/TiO_2$ double layer thin film has the slightly higher roughness with a uniform coating layer.

### 3.3 UV–visible transmittance spectra

Figure 5 shows the UV–visible transmittance spectra for three different thin films. The $SiO_2$ thin films does not exhibit a sharp absorption edge while $TiO_2$ and $SiO_2/TiO_2$ films show a sharp absorption edge in the visible region. The average transmittance of $SiO_2$, $TiO_2$, and $SiO_2/TiO_2$ thin films were 95, 75, and 85 %, respectively. Transmittance is mainly dependent on thickness and surface structure of the thin films. For double layer coating, the transmittance (%) was not significantly different from the

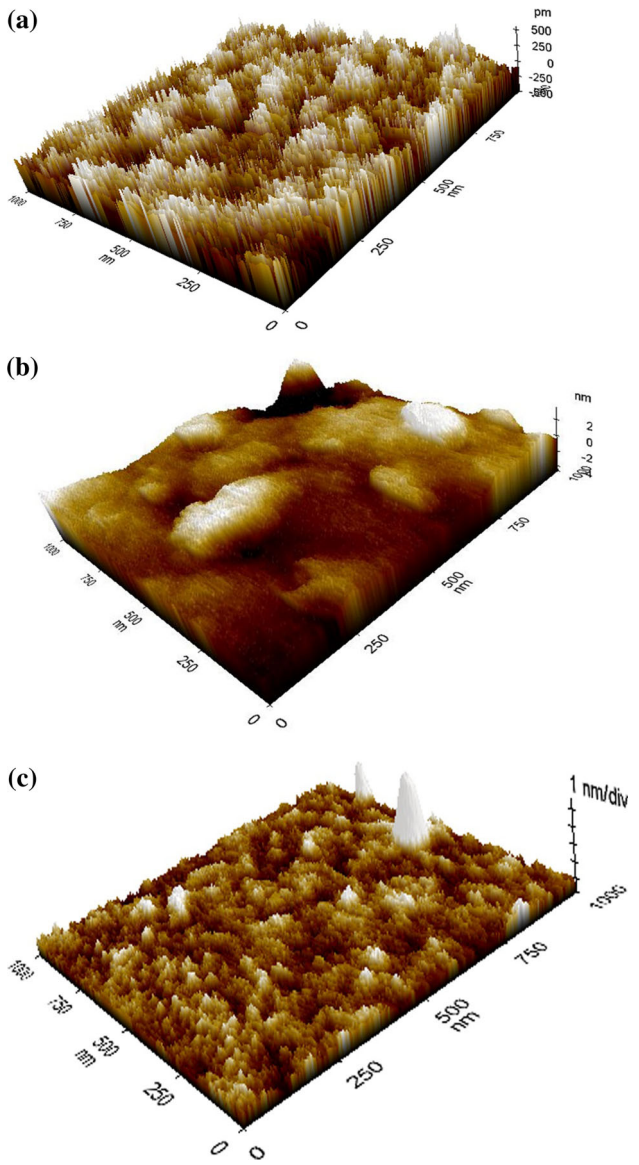


**Fig. 4** AFM images of **a** $SiO_2$, **b** $TiO_2$ and **c** $SiO_2/TiO_2$ thin films

$SiO_2$ coated glass. The transmission of $TiO_2$ decreased by about 10 % comparing to the other glasses. Since anatase $TiO_2$ has a high refractive index (n = 2.52), it reflected a large portion of incident light, resulting in low transmittance [29]. The transmission of the $SiO_2/TiO_2$ double layer thin films was found to be higher than that of a pure $TiO_2$ thin film, due to the decrease of light scattering by the addition of small $SiO_2$ layer [30].

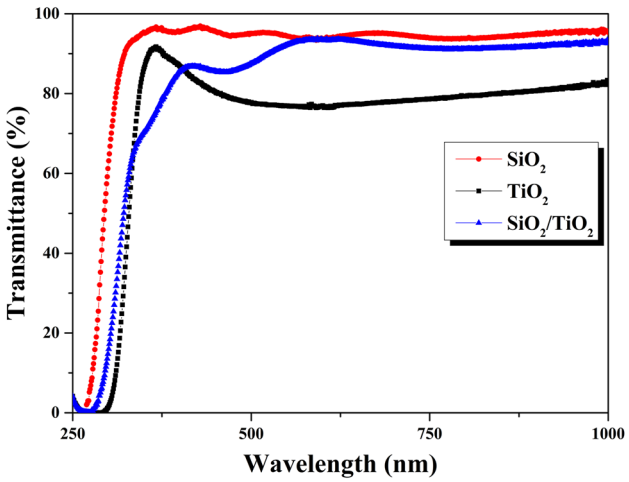


**Fig. 5** Transmittance spectra of $SiO_2$, $TiO_2$, and $SiO_2/TiO_2$ thin films

### 3.4 Hydrophilic and self-cleaning properties

Photo-induced hydrophilic property of the thin films was evaluated by measuring the water contact angle before and after UV irradiation. The water contact angle of the as-prepared $SiO_2$ thin film was 30°. After heat treatment at 400°C, the water contact angle of the thin film was decreased to below 5°. The thermal treatment can eliminate the oxygen defects in the thin film and also enhance roughness [23, 31]. The $SiO_2/TiO_2$ double layer thin films were effectively fabricated by forming the hydrophilic surface of the $SiO_2$ (bottom) layer with thermal treatment. Initially, the water contact angle of $TiO_2$ thin films was 14° and after UV irradiation it decreased to below 5°. In the case of $SiO_2/TiO_2$ double layer thin film, the water contact angle was 24°. Upon UV irradiation, the water contact angle was decreased to 7° and further reached to almost 0° within 10 min of irradiation. This indicates that $SiO_2/TiO_2$ double layer thin films show photo-induced super hydrophilicity (Fig. 6).

Additionally, the photocatalytic performance of the thin films was studied by degradation of an aqueous solution of methylene blue under UV irradiation. Figure 7 shows the photocatalytic performance of the $TiO_2$ and $SiO_2/TiO_2$ thin films as a function of irradiation time. In the absence of thin films, MB solution was stable when irradiated with UV light. Both $TiO_2$ containing thin films were found to be photocatalytically active for the photocatalytic degradation of MB solution under UV light irradiation. The MB

**Table 1** Arithmetic roughness ($R_a$), root-mean-square roughness ($R_{rms}$), skewness ($R_{sk}$) and kurtosis ($R_{ku}$) of the thin films

| Thin films | Roughness $R_a$ (nm) | Roughness $R_{rms}$ (nm) | Skewness $R_{sk}$ | Kurtosis $R_{ku}$ |
|---|---|---|---|---|
| $SiO_2$ | 0.11039 | 0.1378 | −0.125 | 2.945 |
| $TiO_2$ | 0.733 | 0.998 | 0.514 | 5.113 |
| $SiO_2/TiO_2$ | 0.971 | 1.219 | −1.287 | 3.665 |

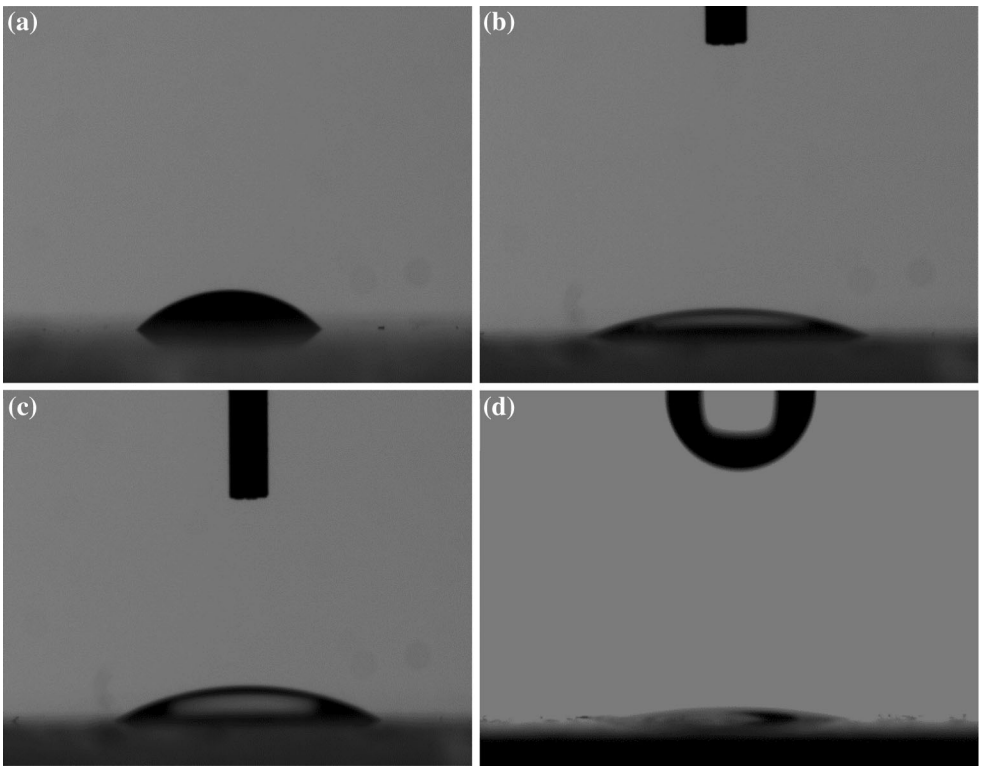


**Fig. 6** Water contact angle measurements for **a** $SiO_2$, **b** $TiO_2$, **c** $SiO_2/TiO_2$ (before UV irradiation), and **d** $SiO_2/TiO_2$ (after UV irradiation)

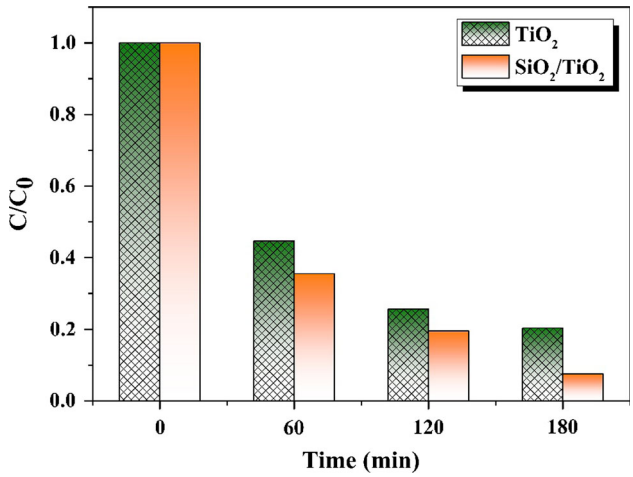


**Fig. 7** Photocatalytic degradation of MB on $TiO_2$ and $SiO_2/TiO_2$ thin films

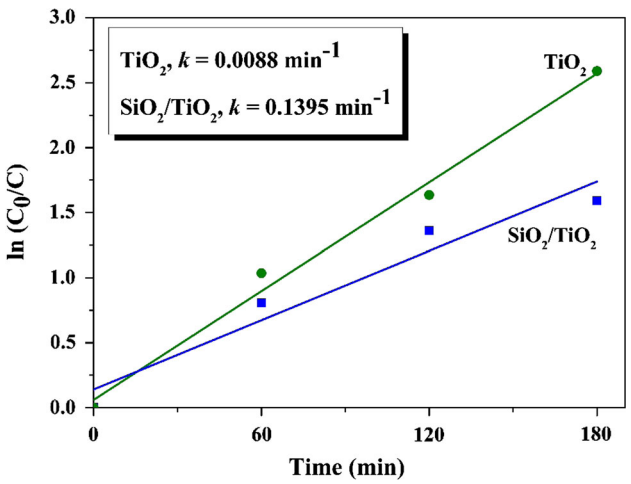


**Fig. 8** The pseudo first order kinetics of degradation of MB over $TiO_2$ and $SiO_2/TiO_2$ thin films

degradation reaction followed pseudo-first order kinetics. The apparent rate constant of the photocatalytic reaction was determined by plotting $\ln(C_0/C)$ against time, where $C_0$ is the initial concentration of MB solution and C is the concentration of MB after irradiation of the thin films in the corresponding time interval (Fig. 8). The reaction rate constants of $TiO_2$ and $SiO_2/TiO_2$ thin films under UV light irradiations were 0.0088 and 0.1395 $min^{-1}$, respectively. The obtained results showed that the photocatalytic performance of $SiO_2/TiO_2$ double layer thin films was superior to single layer $TiO_2$ thin films. The superior photocatalytic activity of $SiO_2/TiO_2$ double layer thin films can be attributed to its higher optical transmission than that of a pure $TiO_2$ thin film. The higher optical transmission of double layer thin films was due to the decrease in light scattering by the addition of thin $SiO_2$ layer. The

combination of low and high refractive materials $SiO_2$ and $TiO_2$ are suitable for a broad range wavelength which increases the spectral bandwidth and has more lifetimes [32]. In addition to these, the changes in microstructure and surface roughness enhance the photocatalytic performance of the $TiO_2$ thin films. As shown in Fig. 4, surface roughness and specific surface area of $SiO_2/TiO_2$ thin films is higher than that of $TiO_2$ only.

## 4 Conclusions

A facile sol–gel coating method has been used for coating $TiO_2$, $SiO_2$, and $SiO_2/TiO_2$ on the glass substrate. The prepared $TiO_2$ and $SiO_2/TiO_2$ thin films are highly transparent and antireflective. The existence of an intermediate $SiO_2$ layer plays a vital role in the photocatalytic performance of the $TiO_2$ thin films coated on glass substrates. The photocatalytic degradation of methylene blue is enhanced because of intermediate $SiO_2$ layer. FE-SEM and optical analysis confirmed the changes in microstructure, surface roughness and optical properties attributed to the superior photocatalytic performance of the $SiO_2/TiO_2$ double layer thin films. This double layered thin films with enhanced self-cleaning and antireflective properties have potential value in the field of energy harvesting as well water and air pollution applications.

**Acknowledgments** This research work was supported by a Grant (14CTAP-C077607-01) from Infrastructure and transportation technology promotion research program funded by Ministry of Land, Infrastructure, and Transport of the Korean government.

## References

1. G. Palmisano, V. Augugliaro, M. Pagliaro, L. Palmisano, Chem. Commun. **33**, 3425–3437 (2007)
2. S.-H. Nam, S.-J. Cho, C.-K. Jung, J.-H. Boo, J. Šícha, D. Heřman, J. Musil, J. Vlček, Thin Solid Films **519**, 6944–6950 (2011)
3. D.P. Macwan, P.N. Dave, S. Chaturvedi, J. Mater. Sci. **46**, 3669–3686 (2011)
4. R. Daghrir, P. Drogui, D. Robert, Ind. Eng. Chem. Res. **52**, 3581–3599 (2013)
5. H.M. Yadav, T.V. Kolekar, S.H. Pawar, J.-S. Kim, J. Mater. Sci. Mater. Med. **27**, 57 (2016)
6. D.M. Blake, P.-C. Maness, Z. Huang, E.J. Wolfrum, J. Huang, W.A. Jacoby, Sep. Purif. Rev. **28**, 1–50 (1999)
7. X. Chen, S.S. Mao, Chem. Rev. **107**, 2891–2959 (2007)
8. U.G. Akpan, B.H. Hameed, Appl. Catal. A Gen. **375**, 1–11 (2010)
9. L. Zhou, S. Yan, B. Tian, J. Zhang, M. Anpo, Mater. Lett. **60**, 396–399 (2006)
10. C.F. Song, M.K. Lü, P. Yang, D. Xu, D.R. Yuan, Thin Solid Films **413**, 155–159 (2002)
11. M. Houmard, G. Berthomé, J.C. Joud, M. Langlet, Surf. Sci. **605**, 456–462 (2011)
12. M. Mazur, D. Wojcieszak, J. Domaradzki, D. Kaczmarek, S. Song, F. Placido, Opto Electron. Rev. **21**, 233–238 (2013)
13. Y. Situ, T. Huang, Y. Chen, W. Huang, H. Huang, Ceram. Int. **40**, 919–927 (2014)
14. H.M. Yadav, T.V. Kolekar, A.S. Barge, N.D. Thorat, S.D. Delekar, B.M. Kim, B.J. Kim, J.S. Kim, J. Mater. Sci. Mater. Electron. **27**, 526–534 (2015)
15. A. Soklič, M. Tasbihi, M. Kete, U.L. Štangar, Catal. Today **252**, 54–60 (2015)
16. H. Dislich, P. Hinz, J. Non Cryst. Solids **48**, 11–16 (1982)
17. Q. Chen, Y. Qian, Z. Chen, W. Wu, Z. Chen, G. Zhou, Y. Zhang, Appl. Phys. Lett. **66**, 1608 (1995)
18. D. Li, M. Carette, A. Granier, J.P. Landesman, A. Goullet, Thin Solid Films **522**, 366–371 (2012)
19. M. Mazur, D. Wojcieszak, D. Kaczmarek, J. Domaradzki, S. Song, D. Gibson, F. Placido, P. Mazur, M. Kalisz, A. Poniedzialek, Appl. Surf. Sci. **380**, 165–171 (2016)
20. D. Eisenberg, H.S. Ahn, A.J. Bard, J. Am. Chem. Soc. **136**, 14011–14014 (2014)
21. A.T. Rajamanickam, P. Thirunavukkarasu, K. Dhanakodi, J. Mater. Sci. Mater. Electron. **26**, 8933–8938 (2015)
22. S.D. Delekar, H.M. Yadav, S.N. Achary, S.S. Meena, S.H. Pawar, Appl. Surf. Sci. **263**, 536–545 (2012)
23. K. Han, J.H. Kim, Appl. Surf. Sci. **263**, 69–72 (2012)
24. M. Mennig, P. Oliveira, H. Schmidt, Thin Solid Films **351**, 99–102 (1999)
25. N.R. Armstrong, C. Carter, C. Donley, A. Simmonds, P. Lee, M. Brumbach, B. Kippelen, B. Domercq, S. Yoo, Thin Solid Films **445**, 342–352 (2003)
26. H.M. Yadav, S.V. Otari, V.B. Koli, S.S. Mali, C.K. Hong, S.H. Pawar, S.D. Delekar, J. Photochem. Photobiol. A Chem. **280**, 32–38 (2014)
27. F. Bensouici, T. Souier, A. Iratni, A.A. Dakhel, R. Tala-Ighil, M. Bououdina, Surf. Coat. Technol. **251**, 170–176 (2014)
28. A.I. Gómez-Varela, Y. Castro, A. Durán, P.A.A. De Beule, M.T. Flores-Arias, C. Bao-Varela, Thin Solid Films **583**, 115–121 (2015)
29. B. Moongraksathum, Y.-W. Chen, J. Sol–Gel Sci. Technol. **77**, 288–297 (2015)
30. R. Fateh, R. Dillert, D. Bahnemann, Langmuir **29**, 3730–3739 (2013)
31. Y.J. Xu, J.X. Liao, Q.W. Cai, X.X. Yang, Sol. Energy Mater. Sol. Cells **113**, 7–12 (2013)
32. N. Lari, S. Ahangarani, A. Shanaghi, J. Mater. Eng. Perform. **24**, 2645–2652 (2015)